

Direct synthesis of dimethyl ether from syngas over mechanical mixtures of CuO/ZnO/Al₂O₃ and γ-Al₂O₃: process optimization and kinetic modelling

Raquel Peláez, Pablo Marín, Salvador Ordóñez*

Department of Chemical and Environmental Engineering, University of Oviedo, Faculty of Chemistry, Julián Clavería 8, Oviedo 33006, Asturias, SPAIN

* Corresponding author: Salvador Ordóñez

Phone: 34-985 103 437, FAX: 34-985 103 434, e-mail: sordonez@uniovi.es

Abstract

This article explores the use of mechanical mixtures of a methanol synthesis catalyst (CuO/ZnO/Al₂O₃) and acid catalysts (γ-Al₂O₃) for enabling the one-step formation of dimethyl-ether from syngas. The study involved the determination of the optimal catalytic system composition and operating conditions in terms of reactant conversion and dimethyl-ether yield. The catalysts mixture that exhibited the best performance consisted of 92.5% wt. of CuO/ZnO/Al₂O₃ (7.5% wt. of γ-Al₂O₃), when operated with an excess of H₂ (H₂/CO > 1.5) and a small amount of CO₂ (4-6%) in the feed. The influence of temperature (250-270°C) was less marked, due to the influence of the equilibrium.

The final purpose of the study of these properties is to develop one of the first kinetic models for the use of mechanical mixtures of commercial catalysts for this reaction. The experimental data were used to fit and validate a kinetic model based on four reactions: synthesis of methanol from CO, CO₂, water gas shift reaction and methanol dehydration. At the studied reaction conditions, synthesis of methanol is kinetically relevant whereas water gas shift reaction and methanol dehydration are close to equilibrium. The inhibition caused by water was also accounted for in the kinetic model.

Keywords: synthetic fuels, renewable fuels, process intensification, mixed catalyst system, fixed-bed reactor, modelling.

1. Introduction

Dimethyl ether (DME) is one of the most promising bioplatform molecule. Its physicochemical properties, like high cetane number and low combustion emissions of soot, CO, hydrocarbons and NO_x, make DME an interesting alternative to replace diesel or LPG fuels. This application as a substitute for diesel has promoted the development of a large number of research studies in last years [1-3]. Moreover, DME can be used as a platform molecule for the synthesis of a wide range of chemicals of high added value, as well as a fuel precursor [4-9] .

DME is produced from synthesis gas, which can be easily obtained by the traditional gasification process using biomass feedstocks [10]. This implies a renewable resource for the process, decreasing its environmental footprint. The traditional DME manufacturing process involves two steps with methanol as an intermediate product. In the first step, methanol is produced from syngas by a synthesis reaction over a metal catalyst (1 and 2), accompanied by the water gas shift reaction, which consumes carbon monoxide (3). Subsequently, methanol is separated and dehydrated in second reactor with an acid catalyst to obtain DME (4).



Recent advances have shown that this process can be carried out in a single reactor more efficiently. Methanol production from syngas is an equilibrium-limited reaction that is carried out at high pressure (50-150 bar) to get competitive conversions. On the contrary, the direct synthesis of DME is an integrated process where methanol synthesis and its dehydration take place in the same reactor. This reduces considerably the methanol concentration and, hence, shifts the equilibrium limitations. This synergy between reactions in the integrated process allows working at higher temperature and lower pressure than the required in the methanol synthesis [10-12]. This implies that the one-step process has lower

capital and production costs and greater energy efficiency than the two-step technology [13-16].

DME direct synthesis from syngas requires the use of catalyst beds with a CO hydrogenation function (for methanol synthesis) and acid sites (for methanol dehydration). A wide number of catalysts has been proposed in the literature [12, 17]. The main objective is to find a stable catalyst with high selectivity to DME. Typically, metallic oxides as CuO, ZnO or Cr₂O₃ are used as metallic function [18, 19]. The most common catalysts for methanol synthesis consist of copper dispersed on metal oxides: Cu-ZnO, Cu-ZnO-Al₂O₃, Cu-ZnO-CrO₃, Cu-TiO₂-ZrO₂, being Cu-ZnO-Al₂O₃ the most employed [12]. Acid catalysts for methanol dehydration are, generally, γ -Al₂O₃, ion cationic exchange resins or acid zeolites (HZSM-5, NaHZSM-5, Ferrierite) [19-21]. Due to its appropriate surface acidity, high activity, and low cost, γ -Al₂O₃ is the most used catalyst for methanol dehydration. It must be taken into consideration that not only the composition of the catalyst plays an important role in the reaction yield, but also the preparation method has an effect on activity and stability [20, 22, 23]. The catalysts for DME synthesis can be hybrid catalysts, result of combining the two separate types of active sites by a simply physical mixing method; or supported bifunctional catalysts, prepared by coprecipitation, impregnation, sol-gel, other wet chemical methods or even more complex methods (e.g. capsule [24]or core-shell catalysts [18, 25]). Sun *et al.* [10] compared the performance of different hybrid and supported bifunctional catalysts prepared by several methods. It includes CuZnAl/H-MFI400 prepared by physical mixture, impregnation, oxalate coprecipitation and coprecipitation-impregnation; CuZnAl/ γ -Al₂O₃ prepared by physical mixture and coprecipitation; capsule catalysts (CuZnAl@HZSM-5 and Pd-SiO₂@HZSM-5) and others such as CuZn/HZSM-5 prepared by sputtering or catalysts including Fe (CuFeZr+HZMS-5). From their results, it can be concluded that the catalyst which allows a better compromise between selectivity and conversion is the catalyst obtained by physically mixing CuO/ZnO/Al₂O₃ and γ -Al₂O₃. The strong interaction between metallic and acidic functions in the bifunctional catalysts prepared by impregnation and co-precipitation of both functions at the same time could lead to lower activity, lower selectivity to DME and poor stability [26, 27].

Most of the available studies base the kinetic modelling of the one-step process on the combination of the available separate models of the methanol synthesis and dehydration

[28, 29]. This is due to the large amount of published scientific literature about the study of the methanol synthesis mechanism. Early kinetic models for this reaction assumed CO to be the source of carbon in methanol and did not account the influence of CO₂ [30]. Later, other authors proposed models which included CO₂ contribution, although CO₂ was not the main reactant [31, 32]. On the opposite, other studies proposed CO₂ as the only carbon source, without effect of CO [33-35]. Graaf *et al.* [36] developed a kinetic model taking into account both CO and CO₂ hydrogenation and the water gas shift reaction, but they do not consider certain surface intermediates which are relevant in more than one reaction. This problem was solved by the model of Vanden Bussche and Froment [37], who developed a kinetic model based on a detailed scheme of the reaction mechanism and assuming CO₂ to be the main carbon source [37]. This is probably one of the latest and most complete studies about the synthesis of methanol over a CuO/ZnO/Al₂O₃ catalyst in gas phase. More recent studies proposed a kinetic model for a three phase methanol synthesis [38], with a Cu/ZnO/Al₂O₃/Zr₂O₃ catalyst [39], or micro kinetic models [40, 41].

Regarding the synthesis of DME from methanol, the kinetics on acidic catalysts has been studied extensively, with different mechanisms and equations proposed. Most of them agree into considering that the reaction follows either Langmuir-Hinshelwood or Eley-Rideal kinetic models. Many of them explain the mechanism and kinetic by employing acid zeolites [42, 43] and resin materials [44, 45] as catalyst. Mollavali *et al.* [46] derived kinetic global reaction equations based on seven elementary reactions. Bercic and Levec [47, 48] assumed a Langmuir-Hinshelwood mechanism with dissociative adsorption of methanol over γ-Al₂O₃ and derived a rate equation which well predicts the behavior of the reaction.

The number of kinetic studies about the process of DME synthesis in one step is very limited. Lu *et al.* [49] proposed a reaction mechanism and kinetics model for the integrated process in a fluidized-bed reactor with a Cu/ZnO/Al₂O₃/HZSM-5 catalyst prepared by coprecipitation deposition method. Based on the analytical results obtained previously by XPS and XANES methods, they developed a mechanism considering the interaction between the catalyst active centers and different key intermediates of reaction, and derived the corresponding kinetic equations for the reactions involved in the process. A two-phase model is shown to simulate the reactor in a good way (plug flow in the bubble phase and fully back-mixed flow in the dense phase). Aguayo *et al.* [50] proposed a kinetic modelling for the integrated

process, considering also the reverse water-gas shift reaction, the formation of C₁-C₁₀ paraffins and water inhibition by adsorption on the catalyst. This model was later improved by incorporating deactivation caused by coke [51]. The model was developed for a CuO-ZnO-Al₂O₃/γ-Al₂O₃ catalyst prepared by wet mixing method in a fixed bed reactor, with the following reaction conditions: 225-325 °C, 10-40 bar, 1.6-57.0 g_{cat} h mol H₂⁻¹. The physicochemical characteristics of this catalyst lead on a significant yield to undesired paraffins (up to 40%).

The scope of this work is to study the role and interaction between metal and acid functions on the direct synthesis of DME from syngas. For this, the catalyst used consists of mechanical mixtures of commercial CuO/ZnO/Al₂O₃ and γ-Al₂O₃ catalysts. Thus, the interaction between the two catalytic functions is different from those previously reported and kinetically modeled. The study involves the determination of the optimal conditions for the reaction in terms of reactant conversion and DME selectivity, and establishes the influence of the main operation variables, such as temperature, pressure, feed composition or the presence of CO₂. Finally, a main goal is to propose and fit to the experimental data an original kinetic model based on all the simultaneous reactions involved in the process.

2. Material and Methods

2.1. Catalysts and chemicals

The CuO/ZnO/Al₂O₃ commercial catalyst used in this work (denoted as METS-1) was supplied by Chempack as 5 mm diameter and 4.8 mm length pellets, with a density of 2365 kg m⁻³ (Cat 1 in this work). The γ-Al₂O₃ catalyst was supplied by BASF as 4.4 mm diameter and 9.1 mm length pellets, with a density of 1066 kg m⁻³ (Cat 2). Both catalysts were grounded and sieved to 100-250 μm and mixed in adequate proportions.

According to the manufacturer indications, the fresh catalyst mixture was pretreated inside the reactor using a gas flow of 4% H₂ (N₂ as balance gas) at 493 K (2 K min⁻¹ until 493 K, holding for 2 h).

The chemicals consisted of gases (H_2 , CO, CO_2 , N_2 , He, air and DME) supplied by Air Liquide in the form of cylinders with purities higher than 99%. Meanwhile, it is also used for calibration anhydrous methanol, supplied by Sigma Aldrich with 99.8% purity.

2.2. Catalyst characterization techniques

The textural properties of fresh and used catalysts were determined by nitrogen physisorption at 77 K in a Micromeritics ASAP 2020 analyzer by the Brunauer–Emmett–Teller (BET) method for the specific surface area, and the Barrett–Joyner–Halenda (BJH) approach to determine the pore volume and diameter.

2.3. Experimental device

The reactor consisted of a stainless steel tube with 7.75 mm inner diameter and 600 mm length. The reactor was isothermally operated by means of an electric furnace that surrounds the reactor tube. Temperature was measured by two thermocouples along the tube wall, the first one placed at 55 mm of the top of the catalyst bed, and with 40 mm of distance between each other; and one thermocouple placed inside the reactor tube, 30 mm below the final of the catalyst bed. The latter was used to control the electric furnace using a PID controller. The inside of the reactor was packed with different layers: from top to bottom, a bed of glass beads (1 mm) to heat the feed to reaction temperature, the catalyst bed (100-250 μm), a small support bed of ground glass (355-710 μm) and a support bed of steel wool. The length of the catalyst section was about 115 mm.

The reactants were mixed at the desired proportions using mass flow controllers (Bronkhorst High-Tech instruments) and the total feed flow rate is varied to achieve different space times. At the reactor outlet, a pressure regulator (back-pressure type) was placed to maintain the reactor at the working pressure (30 bar). The reactor effluent was maintained at 423 K using heating tape, which prevented methanol and water condensation.

The flowsheet of the equipment used to perform the reactions is given as Supplementary Information (Figure S1).

2.4. Analytical and characterization techniques

On-line analysis of the reactor feed and effluent streams was carried out using a Gas Chromatograph (GC Agilent HP 6890N). The GC is equipped with HP Plot Q and HP MoleSieve 5A capillary columns, respectively, used to separate CO₂, DME, methanol and water, and CO, H₂ and N₂. The HP MoleSieve 5A column is connected to a valve which allows its connection or isolation from the system, according to the required analysis. The outlet of the columns is connected to thermal conductivity (TCD) and flame ionization (FID) detectors placed in series. No other compounds, such as alcohols, were detected during reactions. The analysis is carried out according to the following temperature program: 50°C for 3 min, then a ramp of 10°C/min up to 140°C and a second ramp of 30°C/min up to 240°C and hold 2 min; finally, cold down to 50°C at 30°C/min and hold 1 min. The error associated to the analysis (based on the standard deviation) was estimated, by replicating measurements, to be less than 5% per compound.

The results of the analysis were used to calculate conversion of CO (X_{CO}) and product yields (Y_i) according to the following expressions:

$$X_{CO} = 1 - \frac{w_{CO}}{w_{CO\ in}} \quad (1)$$

$$Y_{DME} = \frac{2}{M_{DME}} \frac{w_{DME}}{w_{CO\ in}} \quad (2)$$

$$Y_{CH3OH} = \frac{M_{CO}}{M_{CH3OH}} \frac{w_{CH3OH}}{w_{CO\ in}} \quad (3)$$

$$Y_{CO_2} = \frac{M_{CO}}{M_{CO_2}} \frac{(w_{CO_2} - w_{CO_2\ in})}{w_{CO\ in}} \quad (4)$$

Where w_i and M_i are, respectively, the mass fraction and molar weight of compound i . The mass fraction is used to calculate conversion and yield, instead of mole fraction, due to the important change in density of the reactions.

Water is actually detected in the GC-TCD, but due to the low amount present in the reaction medium it cannot be quantified. However, as it can be seen in the equations above, water concentration is not necessary for conversion and yields calculations. When this value is required for the modelling, it is determined by the total mass balance to the system.

2.5. Experimental program

The synthesis of dimethyl ether from syngas was studied in a continuous fixed-bed reactor operated at isothermal conditions and 30 bar. Firstly, the reactor was operated at constant operating conditions until steady state was achieved, which took at least 50 h, due to initial catalyst stabilization. After this, the operation conditions were varied according to the experimental program.

The process variables considered in the present work are summarized in

Table 1. First of all, the catalyst bed composition (fraction of catalysts) was studied, and then other process variables, such as space time, temperature or feed composition, were also considered.

Table 1. Variables studied in the experimental program.

Variable	Tested values
Fraction of CuO/ZnO/Al ₂ O ₃ , % wt.	70% / 85% / 92.5% / 100%
H ₂ /CO ratio	0.67 / 1.0 / 1.5
CO ₂ , %mol	0 / 6 / 10 / 14
Space time, kg _{cat} h/Nm ³ _{gas}	0.067 - 0.244
Temperature, °C	250 / 260 / 270

2.6. Modelling

The fixed-bed reactor is modelled as an isothermal plug flow reactor. The assumption of plug flow is fulfilled for long beds packed with small particles: bed height/particle diameter > 50 and bed diameter/particle diameter > 10 (this work 460 and 31, respectively) [52].

Due to the stoichiometry of the reactions involved in the synthesis of dimethyl ether from syngas, density cannot be assumed constant. Hence, the following mass conservation equation, based on mass fractions, is considered:

$$m_0 \frac{\partial w_i}{\partial W_{cat}} = M_i \sum_j \nu_{ij} r_{mj} \quad (5)$$

Where m_0 is the total feed mass flow rate, w_i is the mass fraction of compound i , W_{cat} is the total weight of catalyst, M_i is the molecular weight of compound i , ν_{ij} is the stoichiometric coefficient of compound i in reaction j , and r_{mj} is the rate of reaction j per unit weight of catalyst.

The reactions rates are calculated according to the kinetic model. In the present work, the kinetic model of Table 2 is postulated, fitted and validated with experimental data. This model is based on three possible reactions taking place over the CuO/ZnO/Al₂O₃ catalyst: the synthesis of methanol from CO, from CO₂ and the water-gas-shift reaction. These three reactions are related to each other. According to the literature [37], in a mixture of CO and CO₂ the main reaction responsible of the generation of methanol is the synthesis from CO₂. However, the synthesis from CO has also been included to account for the reaction when the feed contains little CO₂ or H₂O. The kinetic expressions have been proposed based on the mechanistic model of Vanden Bussche and Froment [37]. The model is completed with the reaction of methanol dehydration to dimethyl ether over the Al₂O₃ catalyst. The kinetic equation for this reaction is an elementary equation from Bercic and Levec study [48].

The kinetic equations include a term (called DEN) to account for inhibition due to competitive adsorption of reactants or products over the active sites. The most important inhibition is caused by water, DEN = 1 + $K_{H_2O} f_{H_2O}$, which is produced in high amount in the methanol dehydration [37, 50]. As it was mentioned, the partial pressure of water in the experiments was obtained by solving the total mass balance to the reaction system, given the impossibility of its experimental determination.

The fugacities (f_i) appearing in the kinetic equations are calculated from the corresponding fugacity coefficients, which are determined according to the literature [53] using the virial equation of state (*Tsonopoulos method*, [54]).

The equilibrium constants of the kinetic model are calculated using the temperature-dependent expressions provided by Aguayo *et al.*[50]. More details about the equilibrium calculations are available in the Supplementary Information.

Estimated values for the equilibrium constants as well as fugacity coefficients for the most non-ideal conditions of the experiments are included in Supplementary Information (Tables S1 and S2).

The model is solved using MATLAB code, responsible of performing all the calculations and solving the set of ordinary differential equations (ode15s). The fitting of the unknown parameters from the model is accomplished by the least-square method. The objective function of the least-square based regression consisted of three variables: CO conversion, DME selectivity and methanol selectivity. These variables were the dependent variables for which experimental data is readily available from the experiments. The MATLAB function lsqcurvefit using Levenberg–Marquardt algorithm was used. The 95% confidence intervals were calculated with MATLAB function nlpaci, which uses the residuals and jacobian matrix previously calculated by lsqcurvefit.

The optimal reaction conditions to maximize the DME yield are calculated with the MATLAB function fmincon using the Active Set algorithm.

Table 2. Kinetic model for the synthesis of dimethyl ether from syngas on CuO/ZnO/Al₂O₃ and Al₂O₃ catalysts.

Catalyst	Reaction	Kinetic equation
Cat 1	(1) $CO + 2 H_2 \rightleftharpoons CH_3OH$	$r_1 = \frac{k_1}{DEN^3} \left(f_{CO}f_{H_2} - \frac{f_{CH_3OH}}{K_{eq1}f_{H_2}} \right)$
	(2) $CO_2 + 3 H_2 \rightleftharpoons CH_3OH + H_2O$	$r_2 = \frac{k_2}{DEN^3} \left(f_{CO_2}f_{H_2} - \frac{f_{CH_3OH}f_{H_2O}}{K_{eq2}f_{H_2}^2} \right)$
	(3) $CO + H_2O \rightleftharpoons CO_2 + H_2$	$r_3 = k_3 \left(f_{CO}f_{H_2O} - \frac{f_{CO_2}f_{H_2}}{K_{eq3}} \right)$
Cat 2	(4) $2 CH_3OH \rightleftharpoons C_2H_6O + H_2O$	$r_4 = k_4 \left(f_{CH_3OH}^2 - \frac{f_{C_2H_6O}f_{H_2O}}{K_{eq4}} \right)$

* Inhibition term: $DEN = 1 + K_{H_2O}f_{H_2O}$

3. Results and discussion

3.1. Catalyst characterization results

Table 3 sets out the textural properties of the fresh catalyst, mixed and individually, and the catalysts mixtures used during the reactions. It is observed that the mixture of both catalysts, CuO/ZnO/Al₂O₃ and γ-Al₂O₃, has large surface area and high porosity, mainly due to the contribution of the γ-Al₂O₃. When performing pore size distribution by BJH to the mixture of fresh catalysts, a bimodal distribution is observed, in which the first population of pores has a maximum peak at 6.4 nm and another peak at 15.3 nm. According to the individual pore size values of each catalytic function, the first narrow small pore is attributed to γ-Al₂O₃, whereas the second broad large pore is ascribed to CuO/ZnO/Al₂O₃.

The comparison between the properties obtained for the used catalysts and the fresh ones allows concluding that there are no significant surface changes during the reaction. Since the catalyst beds used are large and well mixed, it is assumed that the samples collected after the reaction are representative of the total catalyst bed.

Table 3. Textural properties of the catalysts obtained by nitrogen physisorption

		BET surface (m ² /g)	Pore Volume (cm ³ /g)	Pore Size (nm)	
Cat 1: CuO/ZnO/Al ₂ O ₃		76.6	0.257	15.3	
Cat 2: γ-Al ₂ O ₃		239.9	0.545	6.4	
70% wt. CuO/ZnO/Al ₂ O ₃ + γ-Al ₂ O ₃	Fresh	125.6	0.343	6.4	15.3
	Used	109.4	0.315	6.0	14.9
85% wt. CuO/ZnO/Al ₂ O ₃ + γ-Al ₂ O ₃	Fresh	101.1	0.300	6.4	15.3
	Used	96.4	0.302	6.1	14.9
92.5% wt. CuO/ZnO/Al ₂ O ₃ + γ-Al ₂ O ₃	Fresh	88.9	0.279	6.4	15.3
	Used	84.5	0.289	6.0	15.2

3.2. Direct synthesis of dimethyl ether: catalyst bed composition

The direct synthesis of dimethyl ether is a complex process involving several reactions and hybrid catalyst beds. In order to assess the role of the γ-Al₂O₃ catalyst, the process was studied without γ-Al₂O₃ and with γ-Al₂O₃ homogeneously mixed with the CuO/ZnO/Al₂O₃

catalyst. In both cases, the same amount of the CuO/ZnO/Al₂O₃ catalyst was used (leading to a space time of 0.14 kg CuO/ZnO/Al₂O₃ h/Nm³). In the experiments with γ-Al₂O₃, the reactor was loaded with a mixture of 70% wt. of CuO/ZnO/Al₂O₃ (30% wt. γ-Al₂O₃) with a total space time of 0.20 kg h/Nm³.

The results of the experiments are summarized in Figure 1 for two operating temperatures (250 and 270°C). The stacked bars represent the yields of the different reactions products, dimethyl ether, methanol and carbon dioxide, and the line indicates the conversion of CO (expressions (1) to (4) of the methodology section were used to calculate these parameters from experimental data). Differences between the sum of the yields and CO conversion, which may be attributed to experimental error and unknown secondary reactions, were maintained very low through the experiments, as observed.

The experiments carried out without γ-Al₂O₃ correspond to the traditional process of methanol synthesis, but operated at “unconventional” operating conditions, e.g. 30 bar and H₂/CO = 1.5, instead of > 50 bar and H₂/CO > 2, respectively. As shown, the main product was methanol and only negligible amounts of dimethyl ether ($Y_{DME} < 0.0034$) were observed. Conversion of CO doubled on increasing temperature from 250 to 270°C, but the yield of carbon dioxide increased considerably (attributed to the degradation of methanol).

The use of the γ-Al₂O₃ co-catalyst had a marked effect in CO conversion at both temperatures, in particular at 250°C with an increase of 280%. Thus, the γ-Al₂O₃ catalyzed the reaction of methanol into dimethyl ether, which shifted the equilibrium of methanol synthesis and, hence, increased the conversion of CO in the overall process. The main reaction product was dimethyl ether, followed by important amounts of carbon dioxide. The synthesis of dimethyl ether generates water as by-product, which reacts with carbon monoxide to produce carbon dioxide and hydrogen, according to the water-gas-shift reaction (also catalyzed by CuO/ZnO/Al₂O₃). This is characteristic of the process of direct synthesis of dimethyl ether, and one of the reasons that allows the operation with a syngas feed of high concentration of carbon monoxide. In fact, the extension of the water-gas-shift reaction can be adjusted by means of the feed H₂/CO ratio [17].

As evidenced by the experimental data, almost all methanol reacted to produce dimethyl ether at the considered reaction conditions ($Y_{CH3OH} < 0.01$). This suggests that the γ-Al₂O₃

catalyst is in excess with respect to the CuO/ZnO/Al₂O₃ catalyst, so the following set of experiments was designed to study the influence of the catalysts ratio. As with a 70% of the CuO/ZnO/Al₂O₃ catalyst the reaction had an excess of γ-Al₂O₃, it was considered only to reduce its amount to try to move away towards conditions where the reaction does not reach the equilibrium. Figure 2 includes the results corresponding to fractions from 70% to 92.5% of the CuO/ZnO/Al₂O₃ catalyst (the rest up to 100% corresponds to γ-Al₂O₃); the total amount of catalyst was maintained constant (space time 0.20 kg h/Nm³). The increase in the CuO/ZnO/Al₂O₃ catalyst fraction had an important influence on CO conversion, with increments of 65%-76% at both reaction temperatures (250 and 270°C). This is attributed to the increase of the amount of CuO/ZnO/Al₂O₃ in the mixture. On the contrary, the decrease of the amount of γ-Al₂O₃ resulted in a small increase of methanol yield, though already being very little in comparison to the other products. The yields of dimethyl ether and carbon dioxide both increased in accordance to the increase of conversion. However, the selectivity of these compounds exhibited a trend which is important to point out: on increasing the fraction of CuO/ZnO/Al₂O₃, selectivity of carbon dioxide increased at the expense of dimethyl ether, which decreased 9% at 250°C and 4% at 270°C. Overall, the yield of dimethyl ether increased, but this decrease of selectivity should be taken into account in the composition of the catalyst bed.

The observed trend is confirmed by comparing with the results obtained in other reported studies performed at similar reaction conditions (260°C, 30 bar, 0.2 kg h/Nm³, H₂:CO=1) [55]. The use of a mechanical mixture of the commercial catalysts in a weight ratio of 1:1 (50% wt. of CuO/ZnO/Al₂O₃), resulted in a minor conversion (14%) and greater selectivity to DME (88%), compared with the results provided in this work (conversion 26%, selectivity to DME 69%) for a 70% wt. of CuO/ZnO/Al₂O₃ mixture (250°C, 30 bar, 0.2 kg h/Nm³, H₂:CO=1.5).

Isothermal conditions were confirmed with the temperature profiles measured with the thermocouples during the experiments, i.e., for reactions with 85% wt. CuO/ZnO/Al₂O₃ and 250°C fixed as temperature inside de reactor (thermocouple 3), the temperature profile was 251°C in thermocouple 1 and 253°C in thermocouple 2. When temperature was increased to 260°C (thermocouple 3), the temperature profile was 255°C in thermocouple 1 and 262°C in thermocouple 2; and with 270°C in thermocouple 3, thermocouple 1 showed 268°C and thermocouple 2 measured 270°C.

3.3. Direct synthesis of dimethyl ether: feed composition

This section is devoted to study the influence of feed composition, specifically H₂/CO ratio and CO₂ concentration. These variables have a marked influence on the kinetics, but also on the thermodynamic equilibrium of the reactions involved in this process. The rest process variables were maintained fixed: mixture of 70% wt. of the CuO/ZnO/Al₂O₃ catalyst, space time 0.20 kg h/Nm³, pressure 30 bar and temperature 270°C. Catalytic bed composition has been fixed at 70 % since sensitivity to feed composition changes is larger at this conditions.

The results of the experiments are summarized in Figure 3, in terms of CO conversion and product yields. The feed H₂/CO ratio had a marked influence on CO conversion in the range 0.67 to 1.5 considered in this work. Ratios higher than 1.5 were not considered since if the H₂ content in the feed is too high, the equilibrium of the WGSR reaction is shifted towards the reactants, thus reducing water consumption formed in the DME synthesis.

Consequently, lower yields of DME are obtained, since the methanol dehydration reaction would also be displaced towards the reactants. Under these conditions it has been shown that there is also an increase in the yield to hydrocarbons and light paraffins by hydrocracking reactions [19]. On increasing the feed H₂/CO ratio, the equilibrium of the reactions was shifted to products, leading to an increase on reaction rate and, hence, CO conversion. It should be noted that the stoichiometric H₂/CO ratio for the direct synthesis of dimethyl ether from syngas (overall reaction process, sum of reactions 1, 3 and 4 of Table 2) is 1. On the contrary, the stoichiometric H₂/CO ratio for the methanol synthesis is 2. As mentioned before in section 3.2, the direct synthesis of dimethyl ether from syngas allows the operation with lower H₂/CO ratios, since part of the required H₂ is regenerated “in situ” through the water-gas-shift reaction. The yield of dimethyl ether and carbon dioxide increased in accordance to the increase in CO conversion, but their relative proportions were maintained constant, i.e. selectivity was unaffected by the feed H₂/CO ratio.

The feed CO₂ concentration had an interesting influence on the process: CO conversion and product yields exhibit a maximum when plotted against CO₂ concentration (Figure 3b and Figure 4, respectively for 70% and 85% wt. fractions of CuO/ZnO/Al₂O₃). The presence of this maximum suggests that, at low concentration, CO₂ has a positive influence on reaction rate with respect to the case of feeding only CO and H₂. This finding supports the occurrence of a

reaction mechanism for the methanol synthesis reaction based on CO₂ as the main reactant, rather than CO [37]. According to this, the kinetic model of the methanol synthesis may involve the reaction from CO and CO₂, as presented in Table 2.

At high feed CO₂ concentration, CO conversion decreased, which is explained by the influence of the water-gas-shift reaction: high CO₂ concentration limits the extension of the equilibrium and, hence, the formation of H₂. As a result, the positive effect of CO₂ on reaction rate is hindered by the limitations due to the equilibrium of the water-gas-shift reaction [28]. This interpretation is confirmed when the product distribution is examined: on increasing the feed CO₂ concentration, methanol selectivity increased (from 0.037 to 0.062, for 70% wt. fraction of CuO/ZnO/Al₂O₃), while CO₂ selectivity decreased (from 0.321 to 0.250, for 70% wt. fraction of CuO/ZnO/Al₂O₃). The latter is in agreement with the reduction in the extension of the equilibrium of the water-gas-shift reaction, due to the presence of CO₂. This also produces a reduction in the consumption of the water released in the dimethyl ether synthesis reaction and, hence, in the extension of the equilibrium of this reaction. For this reason, methanol selectivity increased.

To sum up, the feed composition of the syngas has a marked influence on the reactor performance and should be optimized. A high feed H₂/CO ratio is positive for the reaction, due to the excess of H₂. On the contrary, only a small amount of CO₂ on the feed (4-6% mol) exhibits a positive influence.

3.4. Effect of the space time and temperature on the direct synthesis of dimethyl ether

The space time is a process variable used to study the reactor at different throughputs, which is interesting for the scale-up of the process. In this work, the total amount of catalyst was maintained constant ($6 \cdot 10^{-3}$ kg) and the feed molar flowrate was varied to achieve different space times in the range $0.067 - 0.244 \text{ kg}_{\text{cat}} \text{ h/Nm}^3_{\text{gas}}$. The experiments were carried out for two different fractions of catalyst (85% and 92.5% wt. fractions of CuO/ZnO/Al₂O₃) and three temperatures (250, 260 and 270°C). The other operation conditions remained the same: H₂/CO = 1.5, no CO₂ in the feed and pressure 30 bar.

The results of the experiments are shown in Figure 5 and 6. For all the cases, on increasing the space time, CO conversion increased, which means that the overall process is far from equilibrium conditions (at equilibrium, conversion is independent of space time). The equilibrium conversion and yields predicted by the model have been included in the plots as dashed lines; the solid lines correspond to the predictions of the kinetic model (see following section).

Another important process variable is temperature. It should be noted that the maximum operating temperature recommended by the manufacturer for the CuO/ZnO/Al₂O₃ catalyst is 280°C. Above this value, copper sintering may become important. For this reason, in this work, temperature was only varied in the range 250-270°C. The influence of temperature on the overall process is complex, due to the number of reversible reactions involved. Thus, temperature has a positive influence on the reaction kinetics; however, all the reactions are exothermic, so it is expected a negative influence of temperature on the thermodynamic equilibrium. According to the equilibrium calculations of the reaction model (dashed lines of Figure 5), on increasing temperature, CO conversion at equilibrium decreases (from 0.939 at 250°C to 0.881 at 270°C, for example). The decrease (a 6%) is not as high as expected for the individual reaction of methanol synthesis, because the presence of the reaction of dimethyl ether synthesis contributes to shift the equilibrium toward dimethyl ether product.

The influence of equilibrium explains the trends observed in Figure 5 regarding temperature. At low space times, conversion and yield clearly increase on increasing temperature. Since CO conversion is lower at this situation, the system is far from equilibrium and, hence, the positive effect of temperature on the reaction kinetics prevails. On the contrary, at high space times, the system is closer to the equilibrium, so the positive effect on the reaction kinetics is overcome by the equilibrium limitations. For this reason, CO conversion obtained at space time 0.24 kg_{cat} h/Nm³_{gas} is very similar for all the three temperatures: 0.566, 0.573 and 0.567, respectively, for 250, 260 and 270°C. This is an important outcome that should be taken into account for the selection of the operating condition in the scale-up of the process.

3.5. Kinetic modelling

The experiments corresponding only to a fraction of 85% wt. of the CuO/ZnO/Al₂O₃ catalyst have been fitted to the kinetic model of Table 2, according to the equations and procedure described in section 2.6. The obtained fitting parameters and the corresponding confidence intervals are shown in Table 4. The goodness of the fitting can be assessed by the model predictions depicted as solid lines in Figure 4 and 5 and the sum of square errors (SSE) and the regression coefficients (R^2), available in Table S3 of Supplementary Information. The regression coefficients are near to 1 for CO conversion and DME selectivity, whereas the result in the case of methanol selectivity is worse. This is due to the fact that the methanol dehydration reaction is very close to equilibrium in all the experiments performed. The narrow confidence intervals obtained for the kinetic constants are also a proof of the good fitting.

Note that k_1 and k_2 are expressed per mass unit of catalyst 1 (CuO/ZnO/Al₂O₃) while k_4 is expressed per mass unit of catalyst 2 (γ -Al₂O₃).

Table 4. Fitting parameters of the kinetic model of the synthesis of dimethyl ether from syngas of Table 2.

Model parameters	Constant at 250°C (523 K)	Activation energy (kJ/mol)
k_1 , mol kg _{cat1} ⁻¹ s ⁻¹ bar ⁻²	$(6.43 \pm 0.2) \cdot 10^{-7}$	171.8 ± 1.2
k_2 , mol kg _{cat1} ⁻¹ s ⁻¹ bar ⁻²	$(2.55 \pm 0.18) \cdot 10^{-3}$	3.8 ± 0.03
k_4 , mol kg _{cat2} ⁻¹ s ⁻¹ bar ⁻²	8.13 ± 0.27	
K_{H_2O} , bar ⁻¹	19 ± 0.1	

The synthesis of methanol from both CO and CO₂ (reactions 1 and 2 of Table 2) are required to explain the experimental results obtained at the different space times (Figure 5). Thus, at low space time, CO conversion and CO₂ concentration were very low, so the prevailing reaction was the synthesis of methanol from CO. However, on increasing space time (approx. more than 0.15 kg_{cat} h/Nm³), the concentration of CO₂ rose, because it was generated as by-product when the water produced in the methanol dehydration reacted

with CO according to the water-gas-shift reaction. Hence, at high space times, the contribution of CO₂ to the synthesis of methanol increased considerably accounting for 95–99% of reaction rate of methanol at the conditions encountered at the outlet of the reactor. In accordance to these findings, it was also observed that the synthesis of methanol from CO₂ is required in order to explain the sigmoidal shape of the conversion curve of Figure 5, characteristic of autocatalytic systems (i.e. where a product of reaction, CO₂, enhances the reaction rate).

The role of CO₂ in the synthesis of methanol can also be elucidated by means of the experiments carried out at different CO₂ concentration for the present fraction of catalyst (85% wt. of the CuO/ZnO/Al₂O₃), as shown in Figure 4. When a small amount of CO₂ was fed (up to 4%), the conversion of CO increased, which is in agreement with a major contribution of the CO₂ path in the synthesis of methanol. However, this benefit disappeared at high CO₂ feed concentrations (more than 4%), due to the influence on the water-gas-shift reaction. Thus, more CO₂ concentration leads to a water-gas-shift reaction less shifted towards products and, hence, less hydrogen generated and more free water. The latter being negative for the reaction due to inhibition, as explained below.

The experiments carried out at different temperatures allowed the determination of the activation energies of the two methanol synthesis reactions, 171.8 and 3.8 kJ/mol (Table 4). Note that these activation energies do not correspond to a kinetic constant of an elementary reaction step, but to a combination of kinetic constants and (adsorption) equilibrium constants of many elementary steps of the reaction mechanism [37].

The water-gas-shift reaction was in equilibrium at the studied reaction conditions, due to the high activity of the CuO/ZnO/Al₂O₃ catalyst for this reaction (for this reason k₃ is missing in Table 4). This is in agreement with previous studies of this process [50], and can be confirmed by the beta factor obtained in the equilibrium calculations (Supplementary Information).

The reaction of methanol dehydration to dimethyl ether was completely displaced to products: almost all the generated methanol reacted to form dimethyl ether. This behavior suggests that the kinetic constant of this reaction is very high in comparison to the kinetic constants of the methanol synthesis reactions. Only for the case of the lowest space time

(with very low CO conversion), selectivity of methanol was found to be dependent of space time and slightly increased above 5%. Using these data, a kinetic constant of $k_4 = 8.13 \text{ mol kg}_{\text{cat}}^{-1} \text{ s}^{-1} \text{ bar}^{-2}$ was fitted (Table 4), which is a high value, as previously anticipated based on the experimental data (the discrimination of a significant activation energy for k_4 was impossible). For practical purposes, such as the scale-up of the process where space time is high, this reaction can be assumed to be in equilibrium.

Water is generated as by-product in the methanol dehydration reaction, but part of this water reacts with CO to form CO₂ and H₂ according to the water-gas-shift reaction and up to equilibrium conditions. The extent of the water-gas-shift reaction is highly dependent of the concentration of reactants and products and, hence, the extent of the other reactions. For example, at low space time (low CO conversion and absence of CO₂), only a small amount of water is generated, which is expected to almost completely react with the high amount of CO already present. On the contrary, at high space time (high CO conversion and CO₂ present), the water-gas-shift reaction is less displaced towards products, and this results in an increase in water concentration in the gas phase. Water is well known to cause inhibition due to competitive adsorption on the active sites of the catalyst [51]. As a consequence of the higher water concentration, the amount of water adsorbed on the catalyst surface increases and, hence, the rate of the methanol synthesis reaction decreases. According to previous literature studies [37, 50], this decrease can be modelled using the typical competitive adsorption models, in which the denominator of the kinetic equation includes different terms for each inhibitory compound (Table 2).

Another way to change the amount of adsorbed water is by introducing CO₂ in the reactor feed. Thus, when CO₂ concentration increases, the water-gas-shift reaction is less displaced towards products and the concentration of water increases, as explained above for the case of high space time. For this reason, experiments like those of Figure 4 are very interesting to assess to validity of the proposed model. Thus, the fitting of the experiments of Figure 4 and 5 resulted in a water adsorption constant of 19 bar⁻¹.

The extent of external and internal mass transfer limitation were evaluated by the Carberry and Wheeler-Weisz methods. A Carberry number ($Ca = r_{\text{obs}}/K_{G}a_{\text{S}}C_{\text{G}}$) smaller than 0.05 means that diffusional retardation by external mass transport may be neglected. Pore diffusion limitation is negligible for Wheeler-Weisz groups (WW: $\eta\phi^2 = r_{\text{obs}}d_p^2(n+1)/2D_eC_{\text{Sj}}$) smaller

than 0.1. These parameters were estimated for the conditions at which mass and heat transfer are more likely to affect the kinetics: 270°C, no methanol or water, and feed composition for CO hydrogenation ($\text{Ca}=2.7 \cdot 10^{-7}$, $\eta\phi^2=5.6 \cdot 10^{-4}$); and the maximum CO_2 concentration obtained during the experiments for CO_2 hydrogenation ($\text{Ca}=9.8 \cdot 10^{-5}$, $\eta\phi^2=8.4 \cdot 10^{-2}$).

In the same way, several correlations were used to evaluate heat transport ($|\beta_{\text{ex}}\gamma^E \text{Ca}| = |K_G(-\Delta H)C_G E_a \text{Ca} / h R T_G^2| < 0.05$ and $|\beta_{\text{in}}\gamma^E \eta\phi^2| = |D_e(-\Delta H)C_{Sj} E_a \eta\phi^2 / k_e R T_S^2| < 0.05$, for internal and external heat transport respectively). For CO hydrogenation, $|\beta_{\text{ex}}\gamma^E \text{Ca}| = 6.9 \cdot 10^{-5}$ and $|\beta_{\text{in}}\gamma^E \eta\phi^2| = 4.1 \cdot 10^{-3}$ were obtained, whereas for CO_2 reaction the results were $|\beta_{\text{ex}}\gamma^E \text{Ca}| = 3.2 \cdot 10^{-4}$ and $|\beta_{\text{in}}\gamma^E \eta\phi^2| = 1.6 \cdot 10^{-2}$.

Taking into account the values obtained from the mass and heat transport evaluations, it can be discarded the presence of any transport limitation during the process.

3.6. Model validation

The previous model has been validated using the set of experiments corresponding to a fraction of 70% and 92.5% wt. of the $\text{CuO}/\text{ZnO}/\text{Al}_2\text{O}_3$ catalyst. The model has been simulated using the parameters of Table 4 and plotted together with the experimental data. No additional fitting has been carried out in this stage. This way, the capability of model to predict new independent data is tested.

For the case of 92.5% wt. of the $\text{CuO}/\text{ZnO}/\text{Al}_2\text{O}_3$ catalyst, Figure 5, the model is able of predicting the dependence of conversion and yield with space time at all the three temperatures. The regression coefficient ($R^2 = 0.92$) and sum of square errors (SSE = 0.020) are similar to those of 85% wt. of $\text{CuO}/\text{ZnO}/\text{Al}_2\text{O}_3$.

The model has also been used to simulate the experiments carried out with a fraction of 70% wt. of the $\text{CuO}/\text{ZnO}/\text{Al}_2\text{O}_3$ catalyst (solid lines of Figure 3). Like in the previous set of experiments, the model predicts adequate conversion and yields obtained for different feed compositions: H_2/CO ratios and feed CO_2 concentrations. For the latter, the maximum CO conversion, experimentally obtained for low CO_2 concentration, is also predicted by the model.

The validation of the model with additional sets of experiments constitutes a proof of the capability of the model for future applications, such as reactor design, simulation or optimization.

3.7. Optimal reaction conditions

Once the validity of the model has been demonstrated, it has been used to determine optimal operating conditions in order to maximize DME yield. Based on the results of section 3.2, the optimization has been performed for a catalytic bed with a fraction 92.5% wt. of the CuO/ZnO/Al₂O₃ catalyst, which is the one with the highest DME yield. The optimum temperature has turned out to be 250°C. The optimal feed composition, relative to H₂/CO ratio and CO₂ content, has been also determined as function of the space time, as well as its corresponding values of conversion and DME and MeOH yields. The obtained results are shown in Figure 7. Optimization for maximum DME yield as a function of space time. a). Optimized feed composition. b). Optimum conversion and yield. Operating conditions: 92.5%wt CuO/ZnO/Al₂O₃, 30 bar and 250°C.

Obviously, the maximum DME yield is obtained for conditions near the equilibrium, so this is why maximum conversion and yields increase on increasing the space time. Regarding to the feed composition, for low values of the space time, the maximum yield is reached with an excess of CO in the feed, so the optimal H₂/CO ratio is lower than the stoichiometric one. On the contrary, high space times require stoichiometric conditions in the feed, since the amount of reactants that react is higher. On the other hand, the presence of CO₂ in the feed has positive effects at lower space time, but the optimal concentration decreases for higher space times.

Conclusions

The present work had demonstrated experimentally in a continuous fixed-bed reactor the synergic effect achieved by the reactions involved, when hybrid catalyst beds formed by mechanical mixtures of CuO/ZnO/Al₂O₃ and γ-Al₂O₃ are used. The catalyst bed composition with optimum CO conversion and DME yield was the mixture formed by 92.5% wt. of CuO/ZnO/Al₂O₃ and 7.5% wt. of γ-Al₂O₃.

The influence of feed composition, temperature and space time was studied at 30 bar. An excess of H₂ (H₂/CO > 1.5) and a small amount of CO₂ (4-6%) in the feed were found to have a positive effect on reaction rate. Thus, it was demonstrated that CO₂ plays a critical role in the direct synthesis of DME.

The process has been modelled according to a kinetic model considering the four reactions involved. The synthesis of methanol from both CO and CO₂ were found to be important for the kinetic of the reaction. The water gas shift reaction was at equilibrium and the dehydration of methanol very close to equilibrium. The inhibition caused by water was also accounted for. The proposed model was fit and validated with the experimental data of the continuous fixed-bed reactor and used for determining the optimal reaction conditions.

Acknowledgements

This work has been financed by Research Projects of the Regional Government of Asturias (project reference GRUPIN14-078), Spanish Ministry of Economy and Competitiveness (CTQ2014-52956-C3-1-R) and by Blue Plasma Power company. The authors acknowledge Chempack and BASF companies for supplying the METS-1 and γ -Al₂O₃ catalysts respectively. Raquel Peláez acknowledges the Spanish Ministry of Economy and Competitiveness for the PhD grant that supports her research.

References

- [1] T.A. Semelsberger, R.L. Borup, H.L. Greene, Dimethyl ether (DME) as an alternative fuel, *J. Power Sources* 156 (2006) 497-511.
- [2] C. Arcoumanis, C. Bae, R. Crookes, E. Kinoshita, The potential of di-methyl ether (DME) as an alternative fuel for compression-ignition engines: A review, *Fuel* 87 (2008) 1014-1030.
- [3] S.H. Park, C.S. Lee, Applicability of dimethyl ether (DME) in a compression ignition engine as an alternative fuel, *Energy Convers. Manage.* 86 (2014) 848-863.
- [4] G. Cai, Z. Liu, R. Shi, H. Changqing, L. Yang, C. Sun, Y. Chang, Light alkenes from syngas via dimethyl ether, *Appl. Catal., A* 125 (1995) 29-38.
- [5] P. Haro, F. Trippe, R. Stahl, E. Henrich, Bio-syngas to gasoline and olefins via DME – A comprehensive techno-economic assessment, *Appl. Energy* 108 (2013) 54-65.
- [6] Y. Liu, K. Murata, M. Inaba, I. Takahara, Synthesis of ethanol from methanol and syngas through an indirect route containing methanol dehydrogenation, DME carbonylation, and methyl acetate hydrogenolysis, *Fuel Process. Technol.* 110 (2013) 206-213.
- [7] R. Peláez, P. Marín, S. Ordóñez, Synthesis of formaldehyde from dimethyl ether on alumina-supported molybdenum oxide catalyst, *Appl. Catal., A* 527 (2016) 137-145.

- [8] G.P. Hagen, M.J. Spangler, Preparation of polyoxymethylene dimethyl ethers by catalytic conversion of dimethyl ether with formaldehyde formed by dehydrogenation of dimethyl ether, in, BP Amoco Corporation, United States, 2000.
- [9] L. Faba, E. Díaz, S. Ordóñez, Recent developments on the catalytic technologies for the transformation of biomass into biofuels :A patent survey, *Renew. Sustain. Energy Reviews* 51 (2015) 273-287.
- [10] J. Sun, G. Yang, Y. Yoneyama, N. Tsubaki, Catalysis chemistry of dimethyl ether synthesis, *ACS Catal.* 4 (2014) 3346-3356.
- [11] T. Takeguchi, K.-i. Yanagisawa, T. Inui, M. Inoue, Effect of the property of solid acid upon syngas-to-dimethyl ether conversion on the hybrid catalysts composed of Cu–Zn–Ga and solid acids, *Appl. Catal., A* 192 (2000) 201-209.
- [12] G. Bozga, I.T. Apan, R.E. Bozga, Dimethyl Ether Synthesis Catalysts, Processes and Reactors, *Recent Pat. Catal.* 2 (2013) 68-81.
- [13] C. Mevawala, Y. Jiang, D. Bhattacharyya, Plant-wide modeling and analysis of the shale gas to dimethyl ether (DME) process via direct and indirect synthesis routes, *Appl. Energy* 204 (2017) 163-180.
- [14] T. Shikada, Y. Ohno, T. Ogawa, M. Ono, M. Mizuguchi, K. Tomura, K. Fujimoto, Direct Synthesis of Dimethyl Ether from Synthesis Gas, *Stud. Surf. Sci. Catal.* 119 (1998) 515-520.
- [15] T. Shikada, Y. Ohno, T. Ogawa, M. Ono, M. Mizuguchi, K. Tomura, K. Fujimoto, Synthesis of dimethyl ether from natural gas via synthesis gas, *Kinet. Catal.* 40 (1999) 395-400.
- [16] D. Mao, J. Xia, B. Zhang, G. Lu, Highly efficient synthesis of dimethyl ether from syngas over the admixed catalyst of CuO-ZnO-Al₂O₃ and antimony oxide modified HZSM-5 zeolite, *Energy Convers. Manage.* 51 (2010) 1134-1139.
- [17] Z. Azizi, M. Rezaeimanesh, T. Tohidian, M.R. Rahimpour, Dimethyl ether: A review of technologies and production challenges, *Chem. Eng. Process.* 82 (2014) 150-172.
- [18] G. Yang, M. Thongkam, T. Vitidsant, Y. Yoneyama, Y. Tan, N. Tsubaki, A double-shell capsule catalyst with core–shell-like structure for one-step exactly controlled synthesis of dimethyl ether from CO₂ containing syngas, *Catal. Today* 171 (2011) 229-235.
- [19] J. Ereña, R. Garoña, J.M. Arandes, A.T. Aguayo, J. Bilbao, Effect of operating conditions on the synthesis of dimethyl ether over a CuO-ZnO-Al₂O₃/NaHZSM-5 bifunctional catalyst, *Catal. Today* 107–108 (2005) 467-473.
- [20] J.L. Li, X.G. Zhang, T. Inui, Improvement in the catalyst activity for direct synthesis of dimethyl ether from synthesis gas through enhancing the dispersion of CuO/ZnO/γ-Al₂O₃ in hybrid catalysts, *Appl. Catal., A* 147 (1996) 23-33.
- [21] Z. Lei, Z. Zou, C. Dai, Q. Li, B. Chen, Synthesis of dimethyl ether (DME) by catalytic distillation, *Chem. Eng. Sci.* 66 (2011) 3195-3203.
- [22] Q. Ge, Y. Huang, F. Qiu, S. Li, Bifunctional catalysts for conversion of synthesis gas to dimethyl ether, *Appl. Catal., A* 167 (1998) 23-30.
- [23] R. Ahmad, D. Schrempp, S. Behrens, J. Sauer, M. Döring, U. Arnold, Zeolite-based bifunctional catalysts for the single step synthesis of dimethyl ether from CO-rich synthesis gas, *Fuel Process. Technol.* 121 (2014) 38-46.
- [24] G. Yang, N. Tsubaki, J. Shamoto, Y. Yoneyama, Y. Zhang, Confinement effect and synergistic function of H-ZSM-5/Cu-ZnO-Al₂O₃ capsule catalyst for one-Step controlled synthesis, *J. Am. Chem. Soc.* 132 (2010) 8129-8136.
- [25] W. Ding, M. Klumpp, S. Lee, S. Reuß, S. Al-thabaiti, P. Pfeifer, W. Schwieger, R. Dittmeyer, Simulation of one-stage dimethyl ether synthesis over a core-shell catalyst, *Chem. Ing. Tech.* 87 (2015) 702-712.
- [26] M. Cai, A. Palčić, V. Subramanian, S. Moldovan, O. Ersen, V. Valtchev, V.V. Ordomsky, A.Y. Khodakov, Direct dimethyl ether synthesis from syngas on copper–zeolite hybrid catalysts with a wide range of zeolite particle sizes, *J. Catal.* 338 (2016) 227-238.

- [27] S.P. Naik, H. Du, H. Wan, V. Bui, J.D. Miller, W.W. Zmierczak, A comparative study of ZnO-CuO-Al₂O₃/SiO₂-Al₂O₃ composite and hybrid catalysts for direct synthesis of dimethyl ether from syngas, *Ind. Eng. Chem. Res.* 47 (2008) 9791-9794.
- [28] K.L. Ng, D. Chadwick, B.A. Toseland, Kinetics and modelling of dimethyl ether synthesis from synthesis gas, *Chem. Eng. Sci.* 54 (1999) 3587-3592.
- [29] G.R. Moradi, J. Ahmadpour, F. Yaripour, Intrinsic kinetics study of LPDME process from syngas over bi-functional catalyst, *Chem. Eng. J.* 144 (2008) 88-95.
- [30] V.E. Leonov, M.M. Karavaev, E.N. Tsybina, G.S. Petrischeva, Methanol synthesis kinetic, *Kinet. Catal.* 14 (1973) 848.
- [31] K. Klier, V. Chatikavanij, R. Herman, G. Simmons, Catalytic synthesis of methanol from COH₂: IV. The effects of carbon dioxide, *J. Catal.* 74 (1982) 343-360.
- [32] P. Villa, P. Forzatti, G. Buzzi-Ferraris, G. Garone, I. Pasquon, Synthesis of alcohols from carbon oxides and hydrogen. 1. Kinetics of the low-pressure methanol synthesis, *Ind. Eng. Chem. Process Des. Dev.* 24 (1985) 12-19.
- [33] M.A. McNeil, C.J. Schack, R.G. Rinker, Methanol synthesis from hydrogen, carbon monoxide and carbon dioxide over a CuO/ZnO/Al₂O₃ catalyst: II. Development of a phenomenological rate expression, *Appl. Cat.* 50 (1989) 265-285.
- [34] J. Skrzypek, M. Lachowska, H. Moroz, Kinetics of methanol synthesis over commercial copper/zinc oxide/alumina catalysts, *Chem. Eng. Sci.* 46 (1991) 2809-2813.
- [35] V. Mochalin, G. Lin, A. Rozovsky, Kinetic-model of the process of methanol synthesis on the Snm-1 catalyst, *Khim. Prom.* (1984) 11-13.
- [36] G. Graaf, E. Stadhuis, A. Beenackers, Kinetics of low-pressure methanol synthesis, *Chem. Eng. Sci.* 43 (1988) 3185-3195.
- [37] K.M.V. Bussche, G.F. Froment, A steady-state kinetic model for methanol synthesis and the water gas shift reaction on a commercial Cu/ZnO/Al₂O₃ catalyst, *J. Catal.* 161 (1996) 1-10.
- [38] M. Šetinc, J. Levec, Dynamics of a mixed slurry reactor for the three-phase methanol synthesis, *Chem. Eng. Sci.* 56 (2001) 6081-6087.
- [39] H.-W. Lim, M.-J. Park, S.-H. Kang, H.-J. Chae, J.W. Bae, K.-W. Jun, Modeling of the kinetics for methanol synthesis using Cu/ZnO/Al₂O₃/ZrO₂ catalyst: influence of carbon dioxide during hydrogenation, *Ind. Eng. Chem. Res.* 48 (2009) 10448-10455.
- [40] L. Grabow, M. Mavrikakis, Mechanism of methanol synthesis on Cu through CO₂ and CO hydrogenation, *ACS Catal.* 1 (2011) 365-384.
- [41] C. Ovesen, B. Clausen, J. Schiøtz, P. Stoltze, H. Topsøe, J.K. Nørskov, Kinetic implications of dynamical changes in catalyst morphology during methanol synthesis over Cu/ZnO catalysts, *J. Catal.* 168 (1997) 133-142.
- [42] J. Bandiera, C. Naccache, Kinetics of methanol dehydration on dealuminated H-mordenite: Model with acid and basic active centres, *Appl. Cat.* 69 (1991) 139-148.
- [43] S.R. Blaszkowski, R.A. van Santen, Theoretical Study of the Mechanism of Surface Methoxy and Dimethyl Ether Formation from Methanol Catalyzed by Zeolitic Protons, *J. Phys. Chem. B* 101 (1997) 2292-2305.
- [44] K. Klusáček, P. Schneider, Stationary catalytic kinetics via surface concentrations from transient data: Methanol dehydration, *Chem. Eng. Sci.* 37 (1982) 1523-1528.
- [45] S. Hosseininejad, A. Afacan, R.E. Hayes, Catalytic and kinetic study of methanol dehydration to dimethyl ether, *Chem. Eng. Res. Des.* 90 (2012) 825-833.
- [46] M. Mollavali, F. Yaripour, H. Atashi, S. Sahebdelfar, Intrinsic kinetics study of dimethyl ether synthesis from methanol on γ-Al₂O₃ catalysts, *Ind. Eng. Chem. Res.* 47 (2008) 3265-3273.
- [47] G. Bercic, J. Levec, Intrinsic and global reaction rate of methanol dehydration over .gamma.-alumina pellets, *Ind. Eng. Chem. Res.* 31 (1992) 1035-1040.
- [48] G. Bercic, J. Levec, Catalytic dehydration of methanol to dimethyl ether. Kinetic investigation and reactor simulation, *Ind. Eng. Chem. Res.* 32 (1993) 2478-2484.
- [49] W.-Z. Lu, L.-H. Teng, W.-D. Xiao, Simulation and experiment study of dimethyl ether synthesis from syngas in a fluidized-bed reactor, *Chem. Eng. Sci.* 59 (2004) 5455-5464.

- [50] A.T. Aguayo, J. Ereña, D. Mier, J.M. Arandes, M. Olazar, J. Bilbao, Kinetic modeling of dimethyl ether synthesis in a single step on a CuO- ZnO- Al₂O₃/γ-Al₂O₃ catalyst, Ind. Eng. Chem. Res. 46 (2007) 5522-5530.
- [51] I. Sierra, J. Ereña, A.T. Aguayo, M. Olazar, J. Bilbao, Deactivation kinetics for direct dimethyl ether synthesis on a CuO-ZnO-Al₂O₃/γ-Al₂O₃ catalyst, Ind. Eng. Chem. Res. 49 (2010) 481-489.
- [52] H.F. Rase, Chemical reactor design for process plants: principles and techniques, 1st ed., John Wiley & Sons Inc., New York, 1977.
- [53] J.M. Smith, H.C.V. Ness, M.M. Abbott, Introduction to chemical engineering thermodynamics, 6th ed., McGraw-Hill, 2001.
- [54] D.W. Green, R.H. Perry, Perry's Chemical Engineers' Handbook, 8th ed., McGraw-Hill, 2008.
- [55] E.J. Kim, N.K. Park, G.B. Han, S.O. Ryu, T.J. Lee, A reactivity test of Cu-Zn-based catalysts prepared with various precursors and precipitates for the direct synthesis of DME, Process Saf. Environ. Prot. 84 (2006) 469-475.

Figures

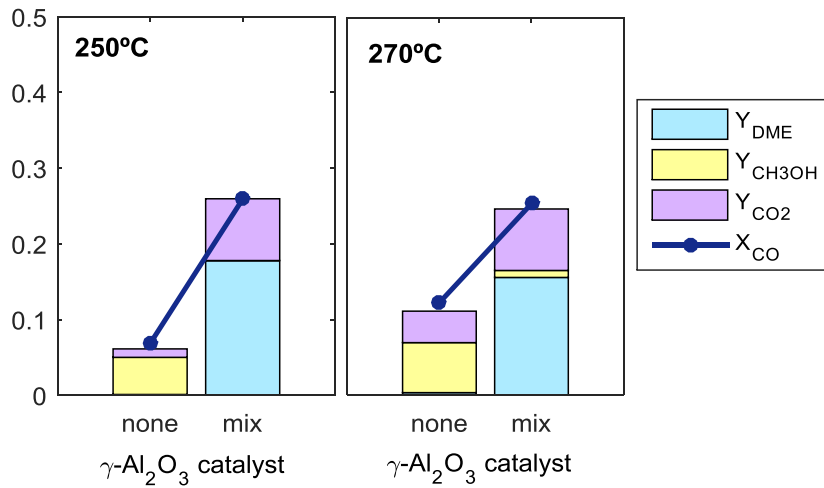


Figure 1. Performance of the reactor equipped with the CuO/ZnO/Al₂O₃ catalyst: without γ-Al₂O₃ and γ-Al₂O₃ homogeneously mixed. Operating conditions: 0.14 kg h/Nm³ (based on CuO/ZnO/Al₂O₃), 30 bar and H₂/CO = 1.50.

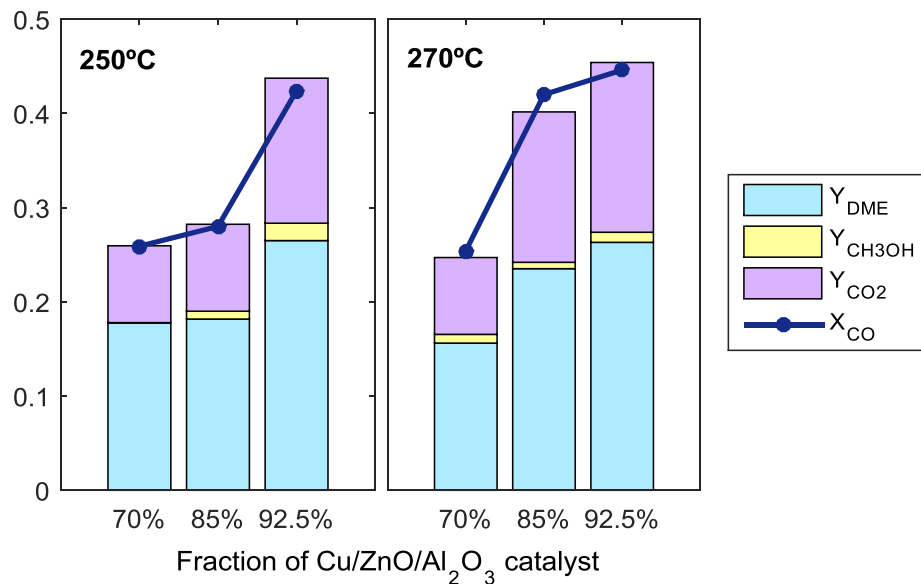


Figure 2. Performance of the reactor for different CuO/ZnO/Al₂O₃ to γ-Al₂O₃ catalyst ratios. Operating conditions: 0.20 kg h/Nm³ (based on total catalyst mixture), 30 bar and H₂/CO = 1.50.

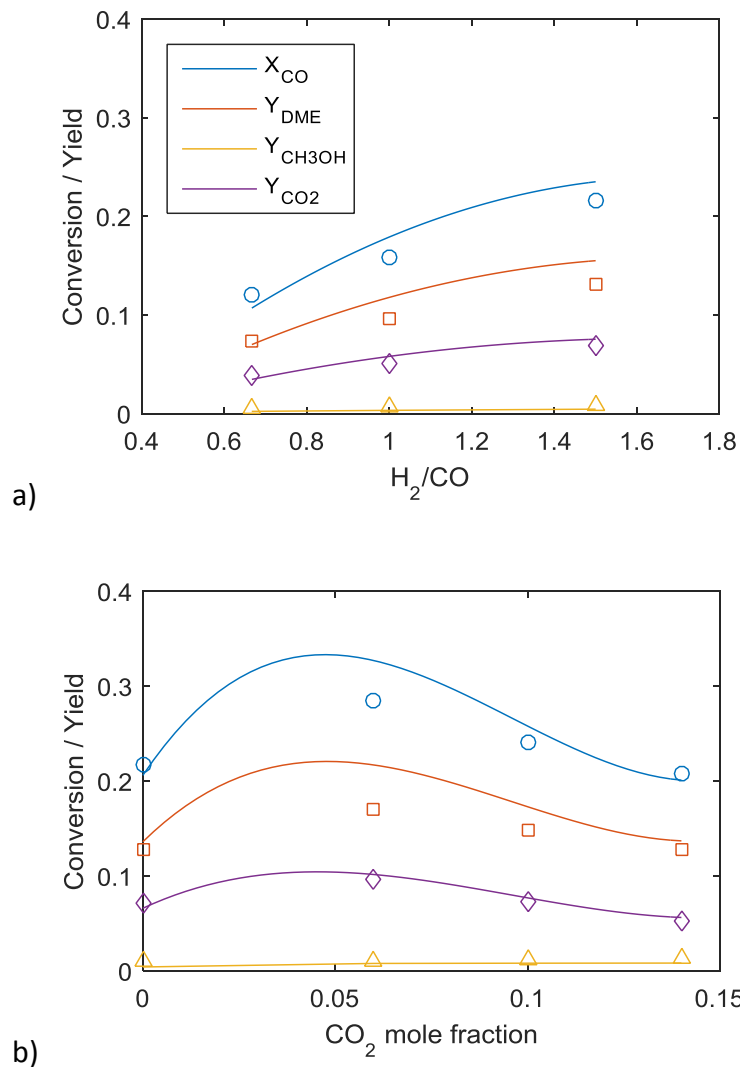


Figure 3. Influence of feed composition on the performance of the reactor: dependence of conversion and yield on H_2/CO ratio (a) and CO_2 feed concentration (b). Operating conditions: $0.20 \text{ kg}_{\text{cat}} \text{ h/Nm}^3$, mixture of 70%wt $\text{CuO}/\text{ZnO}/\text{Al}_2\text{O}_3$, 30 bar and 270°C . Symbols: experiments. (\circ) CO conversion, (\square) DME yield, (\triangle) methanol yield and (\diamond) CO_2 yield. Solid lines: model predictions.

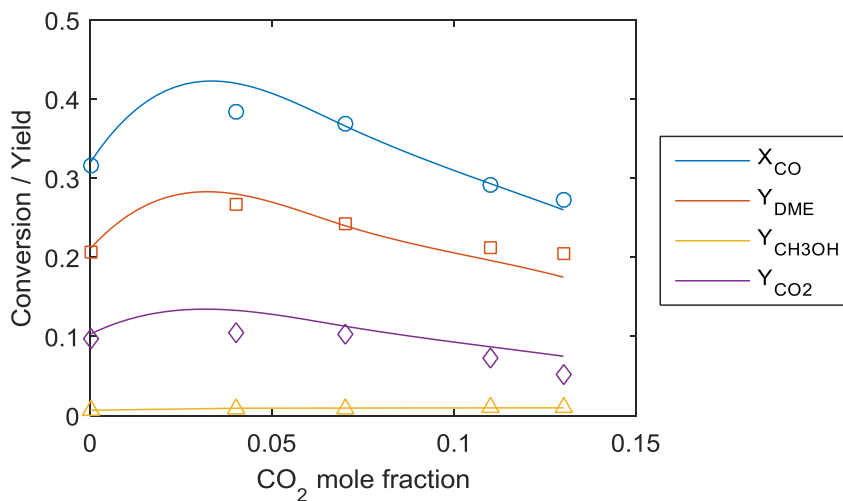


Figure 4. Model fitting for mixture 85%wt CuO/ZnO/Al₂O₃: dependence of conversion and yield on feed CO₂ concentration. Operating conditions: 0.164 kg_{cat} h/Nm³, 270°C, 30 bar and H₂/CO = 1.5. Symbols: experiments. (○) CO conversion, (□) DME yield, (△) methanol yield and (◇) CO₂ yield. Solid lines: model predictions.

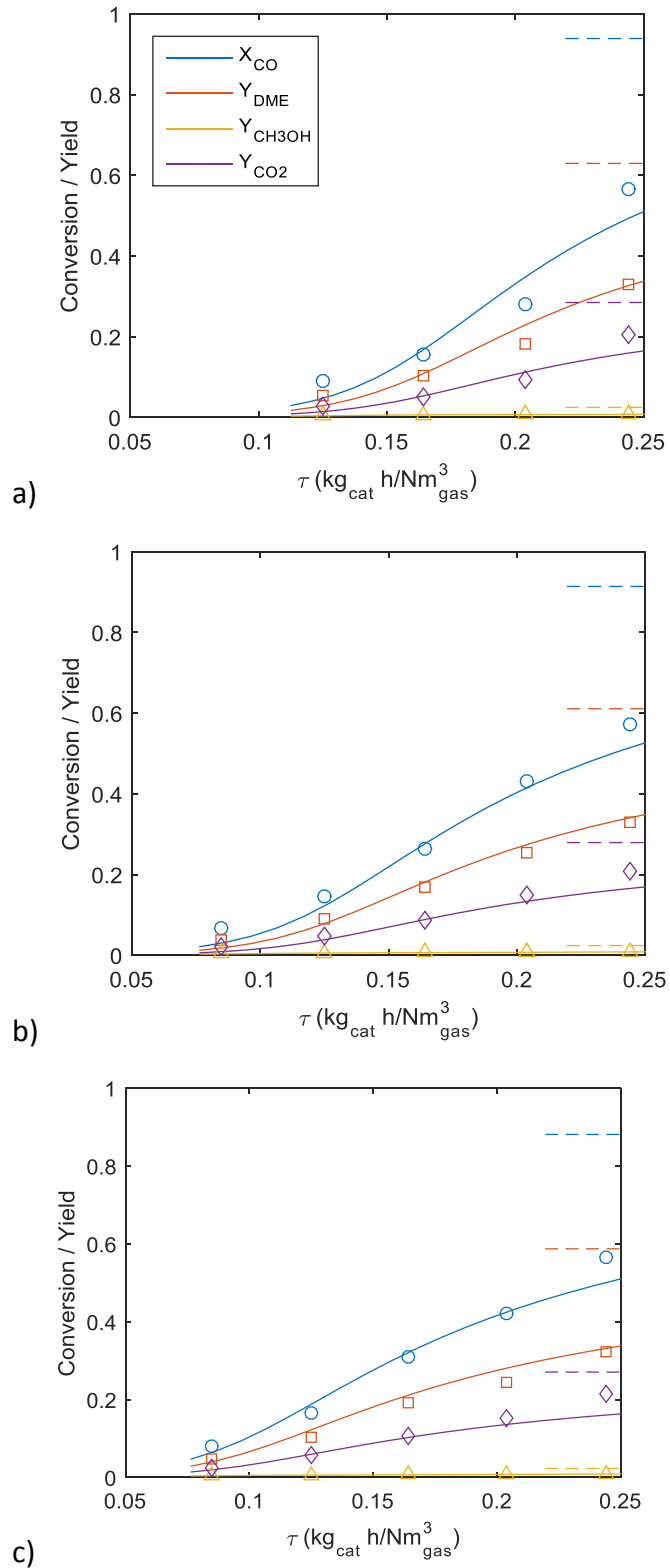


Figure 5. Model fitting for mixture 85%wt CuO/ZnO/Al₂O₃: dependence of conversion and yield on space time at 250°C (a), 260°C (b) and 270°C (c). Operating conditions: 30 bar and H₂/CO = 1.5. Symbols: experiments. (○) CO conversion, (□) DME yield, (△) methanol yield and (◇) CO₂ yield. Solid lines: model predictions. Dashed lines: asymptotic equilibrium value.

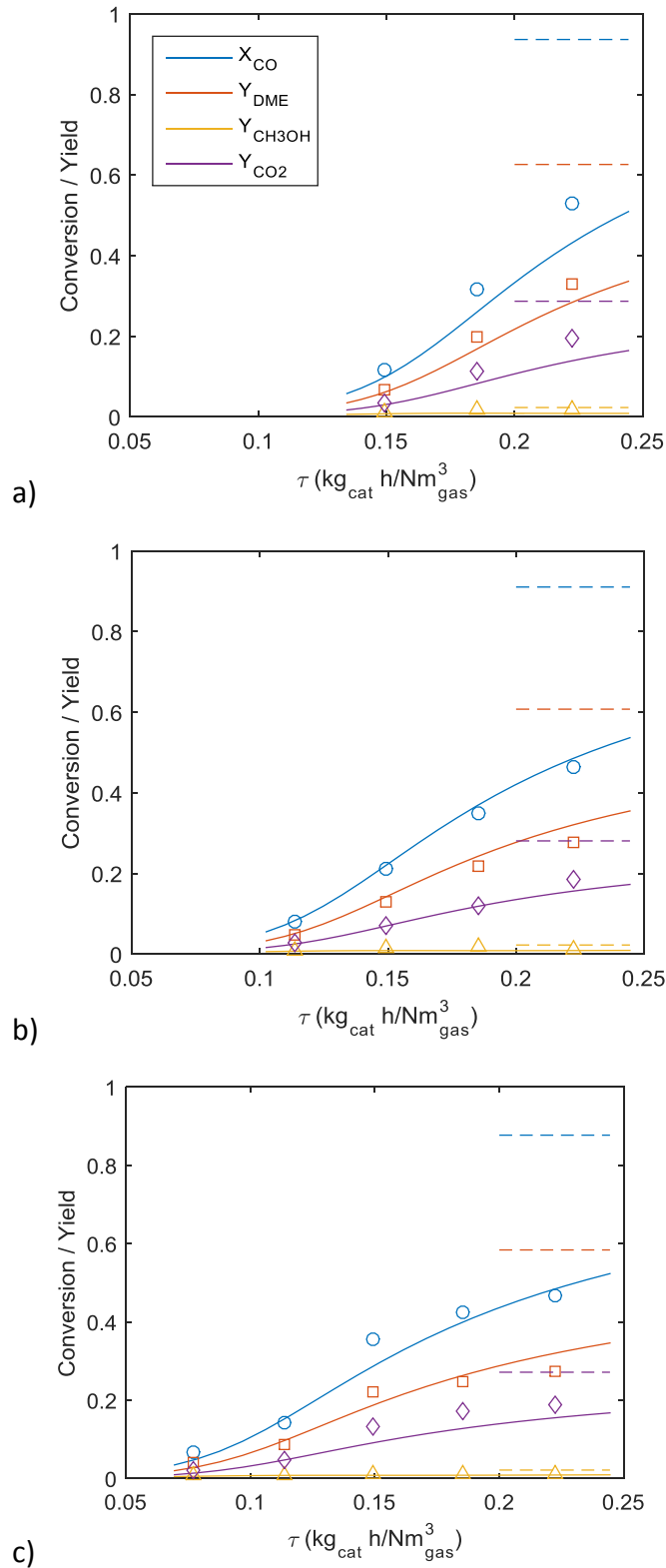


Figure 6. Model validation for mixture 92.5%wt CuO/ZnO/Al₂O₃: dependence of conversion and yield on space time at 250°C (a), 260°C (b) and 270°C (c). Operating conditions: 30 bar and H₂/CO = 1.5. Symbols: experiments. (○) CO conversion, (□) DME yield, (△) methanol yield and (◇) CO₂ yield. Solid lines: model predictions. Dashed lines: asymptotic equilibrium value.

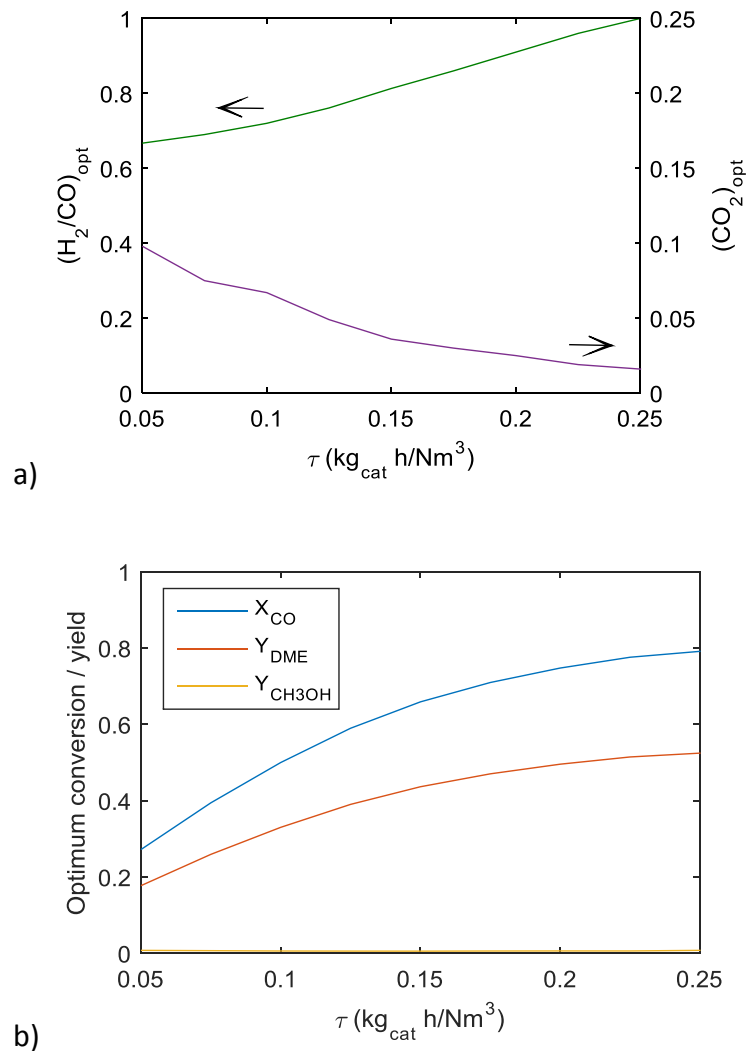


Figure 7. Optimization for maximum DME yield as a function of space time. a). Optimized feed composition. b). Optimum conversion and yield. Operating conditions: 92.5%wt CuO/ZnO/Al₂O₃, 30 bar and 250°C.